# A Wave Optical Algorithm for Hidden-Surface Removal in Digitally Synthetic Full-Parallax Holograms for Three-Dimensional Objects

K. Matsushima and A. Kondoh

Department of Electrical Engineering, Kansai University
Yamate-cho 3-3-35, Suita, Osaka 564-8680, Japan

## ABSTRACT

A novel algorithm is presented for hidden-surface removal in digitally synthetic holograms. The algorithm is able to work with full-parallax holograms and remove obstructed fields in the object wave emitted from three-dimensional (3-D) surface objects. This algorithm is initially discussed as a rigorous procedure to obtain fields behind a tilted planar surface by using the rotational transformation of wave fields, and finally results in the silhouette approximation for reduction of computation time. Reconstructions of holograms created by using the algorithm are demonstrated.

**Keywords:** computer-generated hologram, digitally synthetic hologram, hidden-surface removal, surface model, silhouette approximation

## 1. INTRODUCTION

Algorithms for hidden-surface removal found in literatures on digitally synthetic holograms are either the geometrical method[1,2] or the wave optical method based on layered model.[3] The former is suitable for the ray tracing in the point-source model[4,5] as shown in Fig. 1 (a) but usually much time-consuming algorithm, and therefore it can handle only horizontal-parallax-only holograms. The latter originated in A. W. Lohmann, of which scheme is shown in Fig. 1 (b), has a definite advantage of relatively short computation time owing to utilization of FFT for numerical propagation and is capable of removing fields behind obstacles in full-parallax holograms. The major drawback of the conventional wave-optical method is that the objects must be sliced in some planes parallel to the hologram, and therefore it is difficult to apply standard rendering algorithms necessary for realistic reconstruction of 3-D objects, such as shading and texture mapping.

This report is intended to propose a novel wave-optical algorithm for hidden surface removal. The algorithm is based on a technique to calculate complex amplitude upon tilted plane by the rotational transformation of wave fields[6] and makes it possible to reconstruct a 3-D image with natural overlapping and shading in full-parallax holograms.

## 2. THE WAVE FIELD BEHIND A TILTED SURFACE

### 2.1. Lohmann's layered hologram

The principle of Lohmann's layered hologram and the coordinate system used in this work is shown in Fig. 2. In the coordinates, a hologram is placed in the plane $(\hat{x}, \hat{y}, 0)$ and $\hat{z}$-axis corresponds to the direction of the object wave. It is assumed that incidnet light on a plane V, which is parallel to the hologram at $\hat{z} = \hat{z}_0$, is given as $h(\hat{x}, \hat{y})$. Furthermore, a binary function $\hat{m}(\hat{x}, \hat{y})$ shows whether a location $(\hat{x}, \hat{y})$ on the plane V is included inside the object or not, and is defined as a mask function:

$$\hat{m}(\hat{x}, \hat{y}) = \begin{cases} 0 & \text{(inside object)} \\ 1 & \text{(otherwise)} \end{cases} \tag{1}$$

Further author information: (Send correspondence to Matsushima)
Matsushima: E-mail: matsu@kansai-u.ac.jp, Telephone/Fax: +81-6-6368-0933

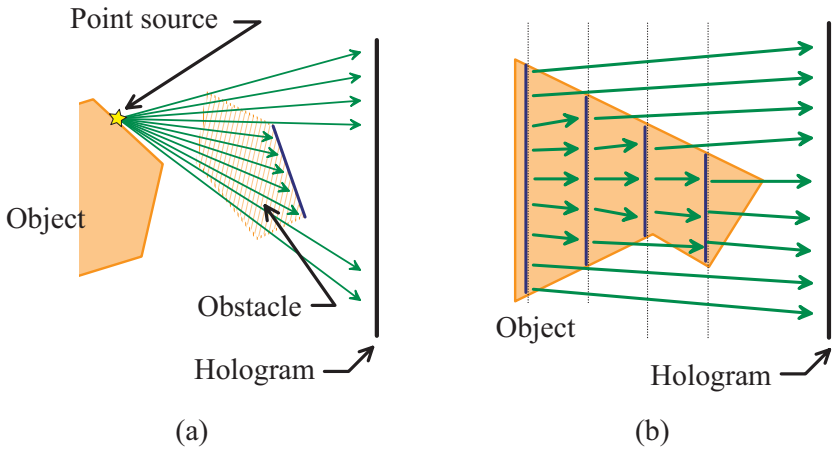


**Figure 1.** Conventional algorithms for hidden-surface removal in digital holograms; (a) geometrical methods; (b) the layered method.

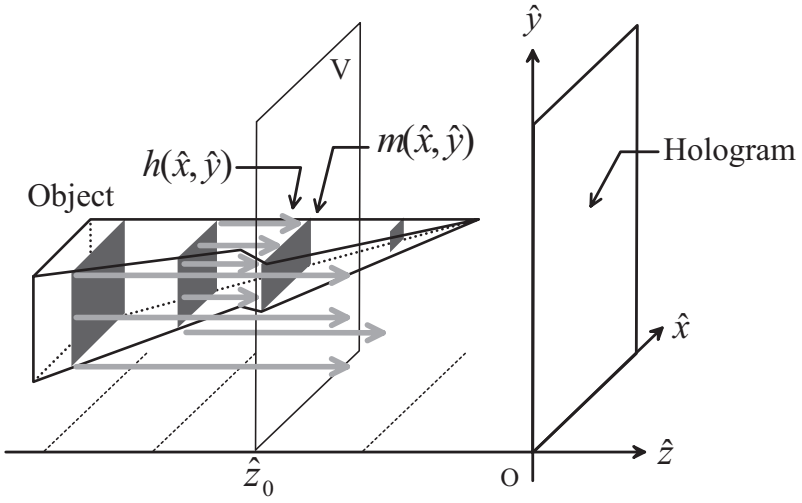


**Figure 2.** The principle of the layered method and the coordinate system used in this work.

This function represents a section of the object. As the incident fields is masked with the section on the plane V, the field behind V is obtained as

$$\hat{h}'(\hat{x},\hat{y}) = \hat{m}(\hat{x},\hat{y})\hat{h}(\hat{x},\hat{y}). \tag{2}$$

Moreover, when it is assumed that the section of object emits the light $o(\hat{x},\hat{y})$, the amount field behind the plane V is given by $\hat{h}'(\hat{x},\hat{y}) + o(\hat{x},\hat{y})$. One can calculates incident fields upon next plane including the next section of object by calculating propagation of the total field $\hat{h}'(\hat{x},\hat{y}) + o(\hat{x},\hat{y})$. Thus, when this procedure is started from the farthest section from hologram and iterated plane by palne to the hologram, we can calculate the object wave without the field propagating inside the object or hiding behind obstacles.

## 2.2. Obstruction of field propagation by tilted planes

It is necessary to handle obstruction of a field by a tilted plane for removing hidden surface of surface-modeled objects composed of small planar surfaces. To consider the procedure for calculating the obstructed field, let us assume that a tilted planar fragment P, which is a part of object surface, hides an incident light $\hat{h}(\hat{x},\hat{y})$ behind the P. We can calculate the obstructed light $\hat{h}'(\hat{x},\hat{y})$ by the following procedure, as shown in Fig. 3.

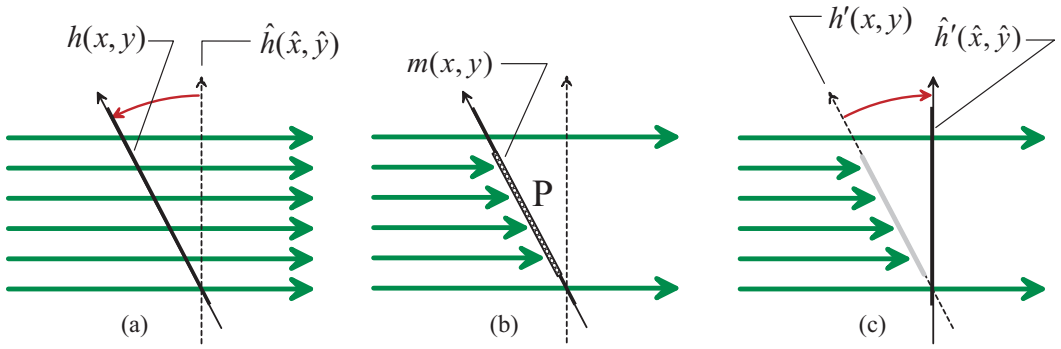


**Figure 3.** The basic procedure for hidden surface removal by employing a wave-optical method. The incident field is obtained upon the object surface by the coordinate rotation in Fourier domain (a) and masked behind the fragment (b). Finally, the fields obstructed are calculated on a plane parallel to the hologram (c).

### Step 1: Calucation of the incidnet field in a tilted coordinates

$h(x, y)$ as well as $\hat{h}(\hat{x}, \hat{y})$ is an incident field but it is given in a tilted coordinates $(x, y, z)$, in which the fragment P is laid upon the $(x, y, 0)$ plane. A method reported in Ref.[6] can be used to obtain the fields $h(x, y)$ from the source fields $\hat{h}(\hat{x}, \hat{y})$ given on the plane parallel to the hologram as summarized bellow.

Spectrum of the field in the tilted plane is obtained as

$$H(u, v) = \mathcal{R}\{\hat{H}(\hat{u}, \hat{v})\}, \tag{3}$$

where $\hat{H}(\hat{u}, \hat{v})$ is Fourier spectrum in the source parallel plane and given as

$$\hat{H}(\hat{u}, \hat{v}) = \mathcal{F}\{\hat{h}(\hat{x}, \hat{y})\}, \tag{4}$$

and $\mathcal{R}\{\cdot\}$ stnads for change of variables for coordinates rotation as follows:

$$\begin{pmatrix} \hat{u} \\ \hat{v} \\ \hat{w} \end{pmatrix} = \mathbf{T} \begin{pmatrix} u \\ v \\ w \end{pmatrix}, \ \mathbf{T} = \begin{pmatrix} \hat{a}_1 & \hat{a}_2 & \hat{a}_3 \\ \hat{a}_4 & \hat{a}_5 & \hat{a}_6 \\ \hat{a}_7 & \hat{a}_8 & \hat{a}_9 \end{pmatrix}. \tag{5}$$

It is noted that the Fourier frequencies are not independent for each other and the relations are given as

$$\hat{w}(\hat{u}, \hat{v}) = \sqrt{\lambda^{-2} - \hat{u}^2 - \hat{v}^2}, \tag{6}$$

$$w(u, v) = \sqrt{\lambda^{-2} - u^2 - v^2}. \tag{7}$$

Complex amplitudes $h(x, y)$ on the tilted plane can be obtained by the following inverse Fourier transformation by using the paraxial approximation.[6]

$$h(x, y) = \mathcal{F}^{-1}\{H(u, v)\}. \tag{8}$$

As a result, the rotational transformation of the incident fields is rewritten as

$$h(x, y) = \mathcal{F}^{-1}\mathcal{R}\mathcal{F}\{\hat{h}(\hat{x}, \hat{y})\}. \tag{9}$$

Consequently, twice FFT and once change of variable are necessary for a rotational transformation of the field. It is noted that the change of variable for rotational transformation requires an interpolation of the field because the transformation causes distortion of the equidistant sampling grid.

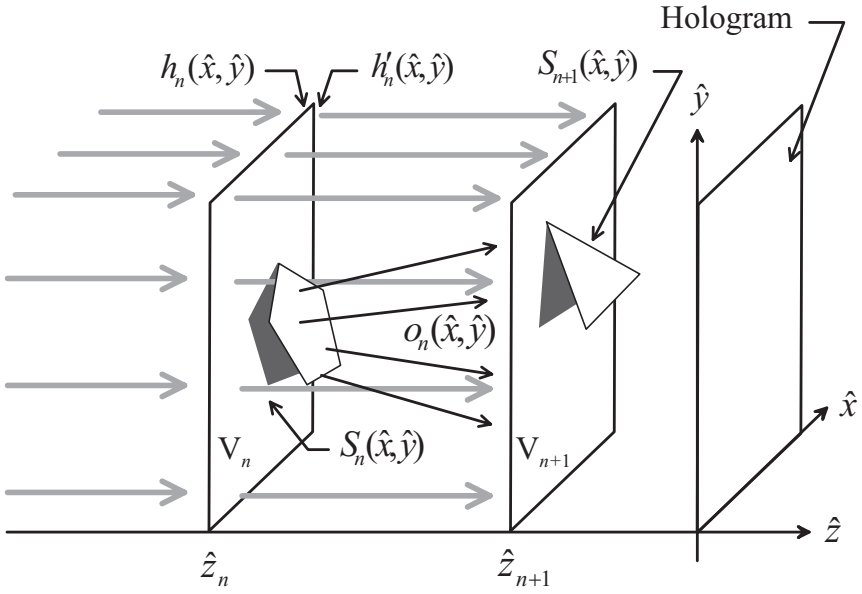


**Figure 4.** Synthesis of the object wave with a wave-optical masking in the silhouette approximation.

**Step 2: Masking the incident field on the tilted plane**

As shown in Fig. 3(b), the fields behind the fragment P is given in the tilted plane as follows:

$$h'(x,y) = h(x,y)m(x,y), \tag{10}$$

where the mask function $m(x,y)$ is again zero in a location included in the fragment P and unity in otherwise.

**Step 3: Inverse rotational transformation of the masked field**

Object waves that propagate almost along $\hat{z}$-axis and reach the hologram are significant for synthesis of object wave. Thus, the field $h'(x,y)$ must be rotated inversely so as to obtain a field upon the plane parallel to the hologram. As a result, the fields obstructed by the fragment P is given by

$$\begin{aligned} \hat{h}'(\hat{x},\hat{y}) &= \mathcal{F}^{-1}\mathcal{R}^{-1}\mathcal{F}\{h'(x,y)\} \\ &= \mathcal{F}^{-1}\mathcal{R}^{-1}\mathcal{F}\left\{\mathcal{F}^{-1}\mathcal{R}\mathcal{F}\{\hat{h}(\hat{x},\hat{y})\}m(x,y)\right\}, \end{aligned} \tag{11}$$

where $\mathcal{R}^{-1}\{\cdot\}$ stands for change of variables for inverse rotation.

## 2.3. The silhouette approximation

Computation time is too long to apply all steps described above to each fragment of the object surface, because four times FFT and twice interpolation is required for handling a fragment. It appears as if it is possible to integrate Step 1 and 3, which is rotation and inverse rotation of a field, and reduce computation time. However, the integration is not easy because of non-linearity of eqs. (6) and (7). Therefore, an approximation should be introduced to the integration.

Fourier frequency $\hat{w}(\hat{u},\hat{v})$ is expanded into power series of $\lambda^{-1}$.

$$\hat{w}(\hat{u},\hat{v}) \simeq \lambda^{-1}[1 - (\lambda\hat{u})^2/2 - (\lambda\hat{v})^2/2] + \cdots \tag{12}$$

If the sampling distance of hologram is much lager than the wavelength, i.e., if the spectral bandwidth of $\hat{h}(\hat{x},\hat{y})$ is far narrower than $\lambda^{-1}$, the field is considered to propagate in almost $\hat{z}$ direction. Therefore, it can be assumed

**Table 1.** Parameters used to synthesize object waves and fabricate holograms.

| | |
|---|---|
| Number of pixels | $8192 \times 4096$ |
| Pixel size | $2\ \mu\text{m} \times 4\ \mu\text{m}$ |
| Reconstruction wavelength | 632.8 nm |

that $\hat{u}, \hat{v} \ll \lambda^{-1}$ and eq. (12) approximate to $\hat{w}(\hat{u}, \hat{v}) \sim \lambda^{-1}$. In that cases, the field behind the fragment is given on a plane parallel to the hologram as follows (see Appendix A):

$$\hat{h}'(\hat{x}, \hat{y}) = m(\hat{a}_1\hat{x} + \hat{a}_4\hat{y}, \hat{a}_2\hat{x} + \hat{a}_5\hat{y})\hat{h}(\hat{x}, \hat{y}). \tag{13}$$

This equation means that the incident field is simply masked by $m(\hat{a}_1\hat{x} + \hat{a}_4\hat{y}, \hat{a}_2\hat{x} + \hat{a}_5\hat{y})$, which corresponds to a silhouette of the fragment given on a plane parallel to the hologram. We refer to this as the silhouette approximation.

## 3. RECURRENCE FORMULA FOR SYSNTHESIZING THE OBJECT WAVE

As shown in Fig. 4, assume that there are planar fragments $\mathrm{P}_1, \cdots, \mathrm{P}_N$ in object space where the index is assigned in the order in which the farther fragment has smaller index, and also assume that there are planes $\mathrm{V}_1, \cdots, \mathrm{V}_N$ parallel to the hologram at $\hat{z}_1, \cdots, \hat{z}_N$, which intersect corresponding fragments with same index. When mask functions $S_n(\hat{x}, \hat{y})$ are defined as silhouettes of fragments given upon $\mathrm{V}_n$, and the subtotal field emited from fragments located further than $\mathrm{V}_n$, i.e. incident field to $\mathrm{V}_n$, is given as $h_n(\hat{x}, \hat{y})$ upon the plane $\mathrm{V}_n$, the field right behind the silhouette mask is obtained by

$$h'_n(\hat{x}, \hat{y}) = S_n(\hat{x}, \hat{y})h_n(\hat{x}, \hat{y}). \tag{14}$$

On the next plane $\mathrm{V}_{n+1}$, the field $o_n(\hat{x}, \hat{y})$ emitted from the surface fragment $P_n$ itself is superimposed on the field $F_{d_n}\{h'_n(\hat{x}, \hat{y})\}$, which is the numerically propagated field of $h'_n(\hat{x}, \hat{y})$. Here, $F_d\{\cdot\}$ denotes a propagation operator for a distance of $d$ and $d_n = |\hat{z}_{n+1} - \hat{z}_n|$. As a result, the next subtotal field on $\mathrm{V}_{n+1}$, including all field emitted from fragments located further than $z_{n+1}$, is wirtten as

$$\begin{aligned} h_{n+1}(\hat{x}, \hat{y}) &= F_{d_n}\{h'_n(\hat{x}, \hat{y})\} + o_n(\hat{x}, \hat{y}) \\ &= F_{d_n}\{h_n(\hat{x}, \hat{y})S_n(\hat{x}, \hat{y})\} + o_n(\hat{x}, \hat{y}). \end{aligned} \tag{15}$$

The starter value of this recurrence formula, which is the field emitted from the furthest fragment, is given as

$$h_2(\hat{x}, \hat{y}) = o_1(\hat{x}, \hat{y}). \tag{16}$$

The object wave is calculated by the recurrence formula (15) in sequence from the starter value, and final field upon the hologram is given as follows:

$$h_{Hologram}(\hat{x}, \hat{y}) = F_{|\hat{z}_N|}\{h_N(\hat{x}, \hat{y})S_N(\hat{x}, \hat{y})\} + o_N(\hat{x}, \hat{y}), \tag{17}$$

where $N$ is the number of fragments constructing the object and $\hat{z}_{N+1} = 0$.

## 4. FABRICATION AND OPTICAL RECONSTRUCTION

Some holograms, of which object waves were synthesized by using eq.(15), were fabricated and optically reconstructed. The common parameters used for calculation and fabrication is shown in Table 1.

Fig. 5 (a) shows a reconstruction of the hologram of a cube placed at $\hat{z} = 100$[mm]. The width of the object is 12mm. In synthesis of the object wave, the object field $o_n(\hat{x}, \hat{y})$ is calculated by the point source method in a density of 2500 point/cm$^2$. Fig. 5 (b) is of three-dimensional characters "KU", of which total width is 12mm

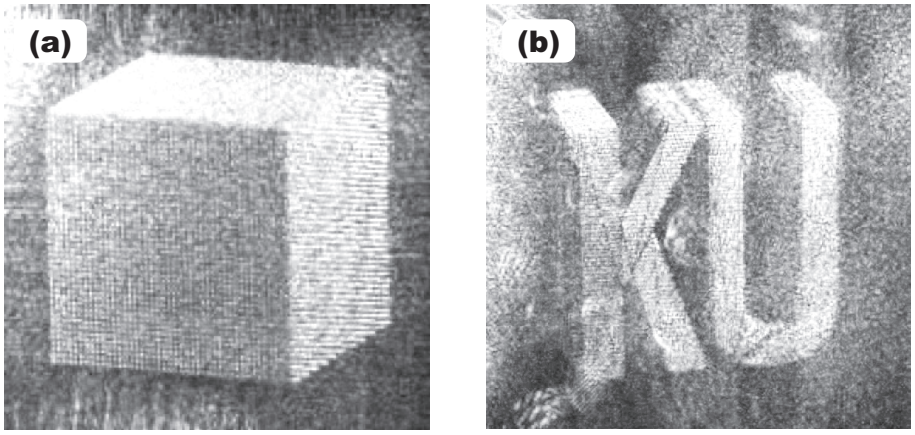


**Figure 5.** Optical reconstruction of holograms of 3-D objects, in which hidden-surfaces are removed by the proposed method; (a) a cube, (b) 3-D characters "KU".

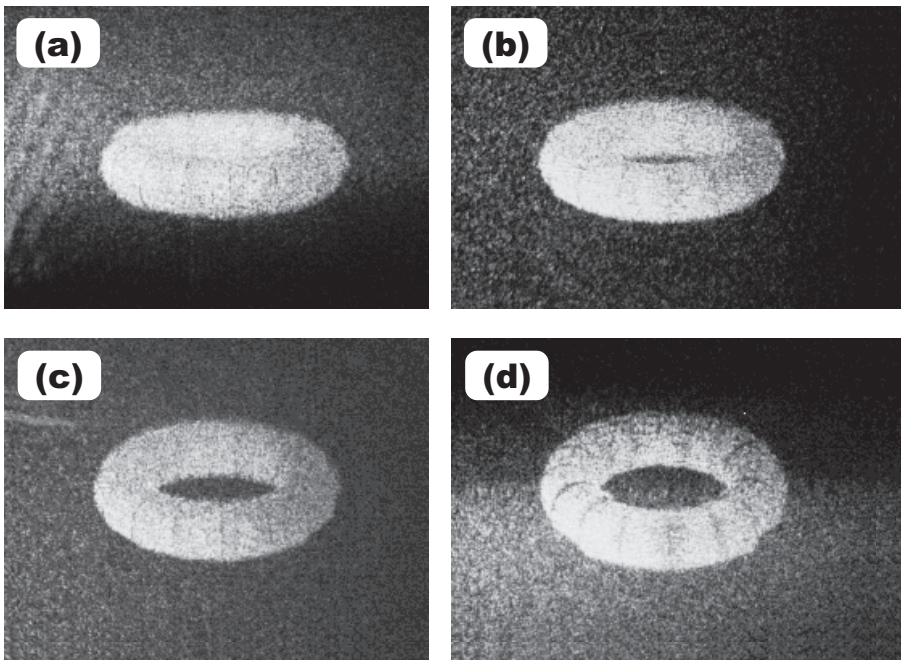


**Figure 6.** Optical reconstructions of the hologram of a torus.

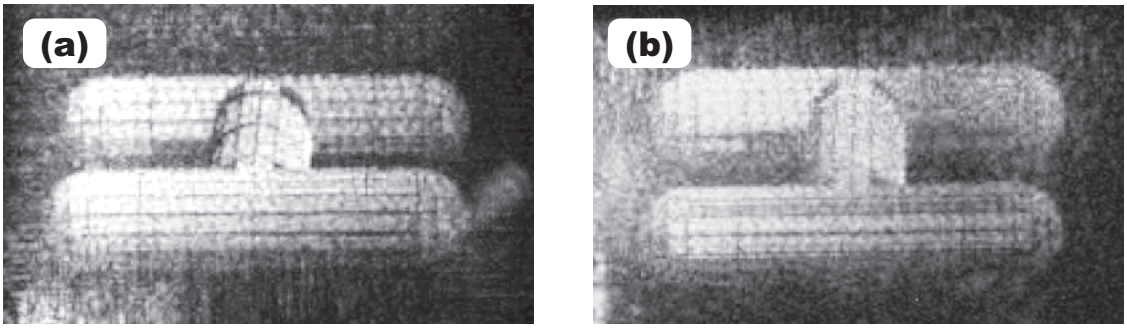


**Figure 7.** Optical reconstructions of a 3-D object constructed of many small planes.

again, but the characters are placed at $\hat{z} = 50$[mm] and the density is 10000 point/cm$^2$. Noted that all of the objects are shaded by flat shading method.

Fig. 6 (a)–(d) show optical reconstructions of the identical hologram of a torus placed at $\hat{z} = 150$[mm], of which diameter is 10mm. The object is constructed of 256 planar fragments and all fragments are composed of point sources in 10000 point/cm$^2$. Heights of the viewpoint is increasing in (a) to (d) and the reconstructed image varies with the heights of the viewpoint, i.e., the reconstructed image has vertical parallax. Fig. 7 (a) and (b) also show reconstructions of a three-dimensional object constructed of many small planar fragments. The height of the viewpoint in (a) is different from that in (b) again.

## APPENDIX A. THE SILHOUETTE APPROXIMATION

Spectrum of the masked field in tilted coordinates is given by Fourier transform of eq.(10):

$$\begin{aligned} H'(u,v) &= \mathcal{F}\{h'(x,y)\} \\ &= \mathcal{R}\{\hat{H}\} * M(u,v), \end{aligned} \tag{18}$$

where $M(u,v)$ is spectrum of the mask function. As Step 3 of Sec.2.2 shown in Fig. 3(c), complex amplitudes of the field on the plane parallel to the hologram is obtained by rotating the spectrum.

$$\begin{aligned} \hat{h}'(\hat{x},\hat{y}) &= \mathcal{F}^{-1}\mathcal{R}^{-1}\{H'(u,v)\} \\ &= \mathcal{F}^{-1}\mathcal{R}^{-1}\{\mathcal{R}\{\hat{H}\} * M(u,v)\}. \end{aligned} \tag{19}$$

When the inverse matrix of eq.(5) is defined as

$$\mathbf{T}^{-1} = \begin{pmatrix} a_1 & a_2 & a_3 \\ a_4 & a_5 & a_6 \\ a_7 & a_8 & a_9 \end{pmatrix}, \tag{20}$$

and assume that only the lowest order in the expansion (12) is significant i.e. higher orders can be ignored, the change of variables is written as follows:

$$\begin{aligned} u &= \alpha(\hat{u},\hat{v}) = a_1\hat{u} + a_2\hat{v} + a_3/\lambda \\ v &= \beta(\hat{u},\hat{v}) = a_4\hat{u} + a_5\hat{v} + a_6/\lambda. \end{aligned} \tag{21}$$

Moreover, the inverse functions are given as

$$\begin{aligned} \hat{u} &= \alpha(u,v)^{-1} = \hat{a}_1 u + \hat{a}_2 v + \hat{a}_3/\lambda \\ \hat{v} &= \beta(u,v)^{-1} = \hat{a}_4 u + \hat{a}_5 v + \hat{a}_6/\lambda. \end{aligned} \tag{22}$$

Eq.(19) is rewritten by use of above functions.

$$\begin{aligned}\hat{h}'(\hat{x},\hat{y}) &= \iint \hat{H}(\alpha^{-1}(u',v'),\beta^{-1}(u',v')) \\ &\times \iint M(\alpha(\hat{u},\hat{v})-u',\beta(\hat{u},\hat{v})-v')\exp[i2\pi(\hat{u}\hat{x}+\hat{v}\hat{y})]\,d\hat{u}d\hat{v}du'dv'. \end{aligned} \tag{23}$$

The variables $(\hat{u},\hat{v})$ of the integration is changed with

$$\begin{aligned} u &= \alpha(\hat{u},\hat{v})-u', \\ v &= \beta(\hat{u},\hat{v})-v', \end{aligned} \tag{24}$$

and furthermore, $(u',v')$ is changed to $(\hat{u}',\hat{v}')$ by eq. (21). As a result, the field on the plane parallel to the hologram is given by

$$\begin{aligned}\hat{h}'(\hat{x},\hat{y}) &= |a_1a_5-a_2a_4||\hat{a}_1\hat{a}_5-\hat{a}_2\hat{a}_4| \\ &\times \iint M(u,v)\exp[i2\pi[(\hat{a}_1\hat{x}+\hat{a}_4\hat{y})u+(\hat{a}_2\hat{x}+\hat{a}_5\hat{y})v]]dudv \\ &\times \iint \hat{H}(\hat{u}',\hat{v}')\exp[i2\pi(\hat{x}\hat{u}'+\hat{y}\hat{v}')]d\hat{u}'d\hat{v}' \\ &= m(\hat{a}_1\hat{x}+\hat{a}_4\hat{y},\hat{a}_2\hat{x}+\hat{a}_5\hat{y})\hat{h}(\hat{x},\hat{y}). \end{aligned} \tag{25}$$

## ACKNOWLEDGMENTS

Authors acknowledge S. Yamanaka and H. Miyauchi for their assistance in fabricating holograms. This work was partly supported by Kansai University High-Technology Research Center.

## REFERENCES

1. J. Underkoffler, "Occlusion processing and smooth surface shading for fully computed synthetic holography," *SPIE Proc. Practical Holography XI* **3011**, pp. 19–29, 1997.
2. T. Hamano and M. Kitamura, "Computer-generated holograms for reconstructing multi-3-D images by space-division recording method," in *Proc. of SPIE*, pp. 23–32, 2000.
3. A. W. Lohmann, "Three-dimensional properties of wave-fields," *Optik* **51**, pp. 105–117, 1978.
4. J. P. Waters, "Holographic image synthesis utilizing theoretical methods," *Appl. Phys. Lett.* **9**, pp. 405–407, 1966.
5. A. D. Stein, Z. Wang, and J. J. S. Leigh, "Computer-generated holograms: A simplified ray-tracing approach," *Computers in Physics* **6**, pp. 389–392, 1992.
6. K. Matsushima, H. Schimmel, and F. Wyrowski, "Fast calculation method for optical diffraction on tilted planes by use of the angular spectrum of plane waves," *J. Opt. Soc. Am.* **A20**, pp. 1755–1762, 2003.